

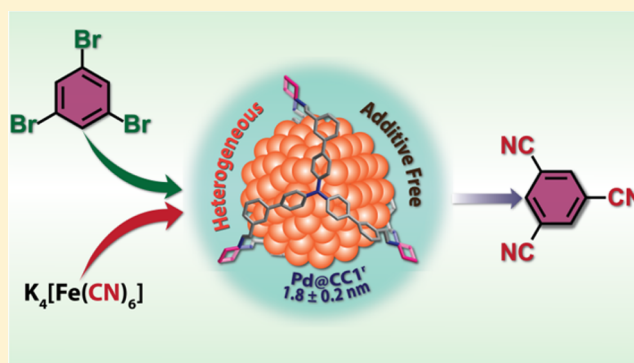
# Molecular Cage Impregnated Palladium Nanoparticles: Efficient, Additive-Free Heterogeneous Catalysts for Cyanation of Aryl Halides

Bijnaneswar Mondal,<sup>‡</sup> Koushik Acharyya,<sup>‡</sup> Prodig Howlader, and Partha Sarathi Mukherjee\*

Department of Inorganic and Physical Chemistry, Indian Institute of Science, Bangalore 560012, India

**S** Supporting Information

**ABSTRACT:** Two shape-persistent covalent cages (CC1<sup>r</sup> and CC2<sup>r</sup>) have been devised from triphenyl amine-based trialdehydes and cyclohexane diamine building blocks utilizing the dynamic imine chemistry followed by imine bond reduction. The cage compounds have been characterized by several spectroscopic techniques which suggest that CC1<sup>r</sup> and CC2<sup>r</sup> are [2+3] and [8+12] self-assembled architectures, respectively. These state-of-the-art molecules have a porous interior and stable aromatic backbone with multiple palladium binding sites to engineer the controlled synthesis and stabilization of ultrafine palladium nanoparticles (PdNPs). As-synthesized cage-embedded PdNPs have been characterized by transmission electron microscopy (TEM), scanning electron microscopy (SEM), and powder X-ray diffraction (PXRD). Inductively coupled plasma optical emission spectrometry reveals that Pd@CC1<sup>r</sup> and Pd@CC2<sup>r</sup> have 40 and 25 wt% palladium loading, respectively. On the basis of TEM analysis, it has been estimated that as small as ~1.8 nm PdNPs could be stabilized inside the CC1<sup>r</sup>, while larger CC2<sup>r</sup> could stabilize ~3.7 nm NPs. In contrast, reduction of palladium salts in the absence of the cages form structure less agglomerates. The well-dispersed cage-embedded NPs exhibit efficient catalytic performance in the cyanation of aryl halides under heterogeneous, additive-free condition. Moreover, these materials have excellent stability and recyclability without any agglomeration of PdNPs after several cycles.



## INTRODUCTION

Over the past two decades, discrete three-dimensional (3D) assemblies have attracted wide interest in many ways, either for their aesthetically elegant architectures or for their remarkable ability to act as sensors,<sup>1</sup> catalysts,<sup>2</sup> and molecular hosts.<sup>3</sup> To this end, numerous shape-persistent discrete assemblies have been devised mainly by articulating organic spacers with appropriate metal centers.<sup>4,5</sup> In contrast, construction of such architectures by using traditional covalent synthesis is undoubtedly more challenging owing to the laborious multiple synthetic steps. However, dynamic covalent synthesis<sup>6</sup> has emerged as an efficient strategy for their easy access, which has been manifested in several recently developed cage compounds.<sup>7</sup> Our group has demonstrated that such an organic architecture could be constructed even from a complex reaction mixture by virtue of dynamic imine bonds.<sup>8</sup> The well-defined pore structures of such materials have been exploited for the gas adsorption/separation; however, they are yet to be explored in detail for the synthesis and stabilization of metal nanoparticles (MNPs).<sup>9</sup>

MNPs enjoy high surface-to-volume ratios with large numbers of available active catalytic sites per unit area, which is believed to be responsible for their higher catalytic performance compared to their bulk metal counterparts.<sup>10</sup> Unfortunately, during catalytic reactions, such small MNPs lose their catalytic activity as a consequence of the formation of aggregates owing to their

high surface energy.<sup>11</sup> Therefore, to deal with this difficulty, a number of different solid support materials, like metal oxides,<sup>12</sup> metal–organic frameworks,<sup>13</sup> polymeric organic frameworks,<sup>14</sup> and so on, have been tested over the past few years.

In the case of porous architectures, the confined nanopores serve as templates to synthesize NPs of different shapes and sizes. It is worth mentioning here that MNPs' size, morphology, and interaction with the solid support have paramount influence on their catalytic activity.<sup>10f,14a</sup> In spite of substantial progress in this field, precise control over the size of the MNPs, and thus fine-tuning of their catalytic activity, is still a grand challenge. Though several discrete architectures of Pd(II)/Pt(II)/Ru(II)/Fe(II) have been explored in recent times for various purposes, they have not been explored as templates/supports for the synthesis of MNPs due to their high vulnerability toward reducing agents.<sup>5h</sup> Therefore, in this context, shape-persistent organic cage compounds, owing to their well-defined geometry, solution processability, structural tunability, and chemical and thermal stability, may bring new opportunities. We envision that nano-organic cage compounds bearing vicinal diamines could be ideal candidates for controlled synthesis of palladium nanoparticles

Received: December 21, 2015

Published: January 15, 2016

(PdNPs). Moreover, such organic-cage-anchored PdNPs may be amenable for heterogeneous/homogeneous catalysis.

The heterogenization of homogeneous catalytic reactions is a major area of research in the pharmaceutical and fine chemical industries.<sup>10e</sup> Heterogeneous catalysts are often less active than their homogeneous counterparts. However, they provide easy catalyst recycling and separation from the reaction mixture, which is particularly important for industrial-scale application of precious metal catalysts.

Herein, we report organic amine cage compounds (Figure 1) as novel platforms for the size-controlled synthesis of PdNPs.

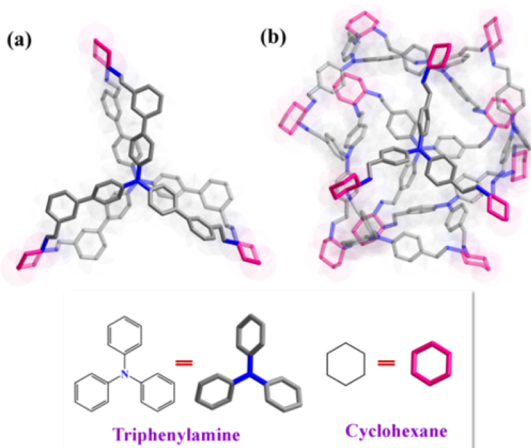


Figure 1. Shape-persistent organic cage compounds (a) CCI<sup>1f</sup> and (b) CC2<sup>f</sup>.

Furthermore, such cage-anchored PdNPs are utilized as heterogeneous catalysts and exhibit superior catalytic performance over some well-known palladium catalysts in the cyanation of aryl halides under heterogeneous, additive-free conditions.

## RESULTS AND DISCUSSION

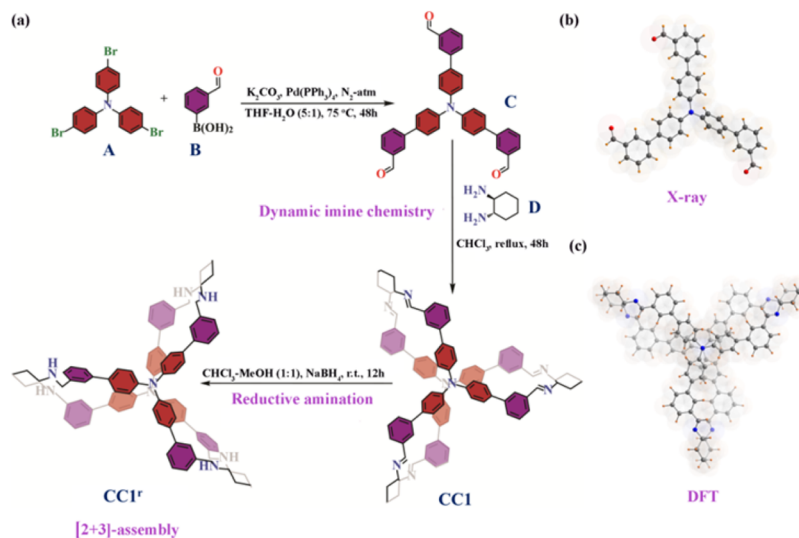
**Synthesis and Characterization of the Cage Compounds.** Purely organic trigonal-prismatic cages are relatively uncommon, although they are one of the simplest possible

architectures known to date. The shape-persistent prismatic CCI<sup>1f</sup> was easily obtained (~80% yield) via the reaction of a triphenyl amine-based trialdehyde C with a chiral diamine D [(*S,S*)-1,2-cyclohexanediamine]. The aldehyde building block C was synthesized by palladium-catalyzed Suzuki–Miyaura cross-coupling reaction of tris(4-bromophenyl)amine (A) and 3-formylphenylboronic acid (B) (Scheme 1). The imine-based cage compound CCI was isolated as a pale yellow solid by treating C with D in a 2:3 stoichiometric ratio in chloroform under reflux for 48 h. The dynamic nature of imine bonds ensures the formation of the thermodynamically most stable product in equilibrium, which herein involves condensation between 3 equiv of diamine and 2 equiv of trialdehyde. Among all the possible architectures, the molecular prism is enthalpically favored owing to its having the least angle strain, as well as entropically favored as it comprises a minimum number of building blocks.<sup>7k</sup> The CCI was transformed into the more stable amine cage CCI<sup>1f</sup> by sodium borohydride reduction of the dynamic imine bonds. As-synthesized CCI<sup>1f</sup> was characterized by multinuclear NMR (<sup>1</sup>H, <sup>13</sup>C), <sup>1</sup>H–<sup>1</sup>H COSY, <sup>1</sup>H–<sup>13</sup>C HMQC, FTIR, and ESI-MS analyses. In the ESI-MS spectrum (Figure 2), peaks at *m/z* 1361.7697 and 681.3862, corresponding to [M+H]<sup>+</sup> and [M+2H]<sup>2+</sup>, respectively, unambiguously advocate for the formation of a [2+3] assembled cage.

Several attempts of crystallization so far have been unsuccessful. However, gas-phase DFT (B3LYP/6-31G) calculation reveals that, in the lowest energy conformer of CCI<sup>1f</sup>, the top and bottom panels of the prism are in skew conformation, in which the distance between the nitrogen atoms of the triphenyl amine core is ~0.8 nm, whereas the distance between the two farthest points inside the cage is ~2.0 nm (Figure S18).

The CC2<sup>f</sup> has been synthesized following the same synthetic protocol as employed for CCI<sup>1f</sup>, from tris(4-formylphenyl)amine (E) and diamine D (Schemes 2 and S1). In ESI-MS spectrum peaks at *m/z* = 1809.4406 and 1206.7337, corresponding to [M+2H]<sup>2+</sup> and [M+3H]<sup>3+</sup> (Figure S22), respectively, indicate that 8 equiv of trialdehyde and 12 equiv of diamine condensed to form a [8+12] cage compound isomeric to the one Cooper et al. obtained using (*R,R*)-1,2-cyclohexanediamine.<sup>15</sup> Gas-phase DFT calculation suggests that this distorted cubical cage compound

Scheme 1. (a) Synthetic Routes for the Synthesis of Trialdehyde C and Molecular Prism CCI<sup>1f</sup>, (b) X-ray Crystal Structure of C, and (c) Gas-Phase DFT (B3LYP/6-31G)-Optimized Structure of the Imine Cage CCI



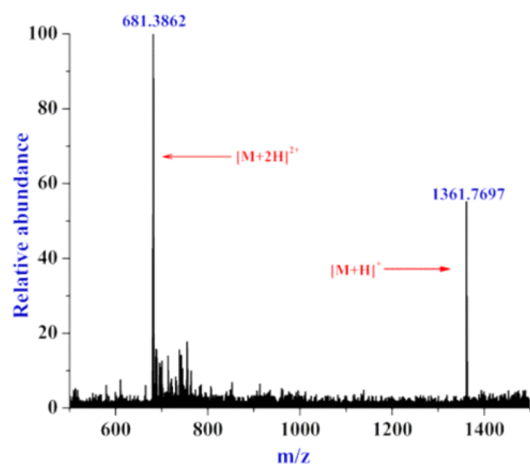
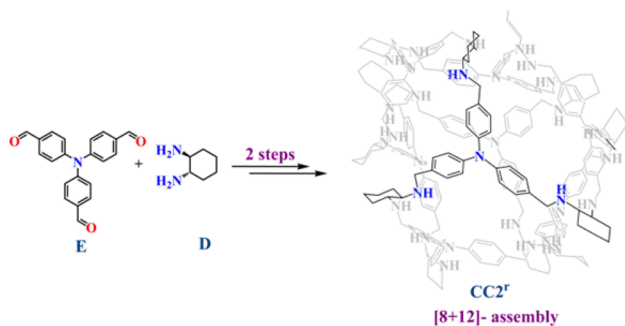


**Figure 2.** ESI-HRMS spectrum of  $\text{CCI}^{\text{f}}$  recorded in  $\text{CHCl}_3$ – $\text{CH}_3\text{CN}$  (1:1; v/v).

**Scheme 2. Synthesis of [8+12] Assembled Covalent Architecture  $\text{CC}2^{\text{f}}$  from Trialdehyde E and Diamine D**



has an internal cavity of  $\sim 2.4$  nm with an outer diameter of  $\sim 3.0$  nm.<sup>15</sup>

**Synthesis of Cage-Anchored Palladium Nanoparticles.**

Compounds having vicinal diamine moieties are suitable candidates for complexation with palladium(II) salts. Therefore,  $\text{CCI}^{\text{f}}$ / $\text{CC}2^{\text{f}}$  furnished with secondary amine moieties could bind with  $\text{Pd}^{2+}$  ions, and such a strong interaction is expected to foster controlled growth and stability of PdNPs.

In view of this fact,  $\text{CCI}^{\text{f}}$  was first reacted with 3 equiv (corresponding to three diamine clefts) of  $\text{Pd}(\text{OAc})_2$  in chloroform. A pale yellow solution of  $\text{CCI}^{\text{f}}$  was treated with an orange-yellow solution of  $\text{Pd}(\text{OAc})_2$  at room temperature, which resulted in a sharp color change from yellow to deep brown (Figure S23), most likely due to complexation of the diamine moieties of the cage with the  $\text{Pd}^{2+}$  ions.

This reaction mixture was subsequently reduced with a methanolic solution of sodium borohydride. The brown solution immediately turned to black without forming any precipitates, which indicates an efficient reduction of  $\text{Pd}^{2+}$  ions into  $\text{Pd}^0$  and further their stabilization by the cage compound. The  $\text{Pd@CCI}^{\text{f}}$  was obtained as a black powder after complete removal of the solvent. Notably, this material was found to be soluble only in  $\text{CHCl}_3$ – $\text{MeOH}$  solvent mixture and stable over a period of days without agglomeration or any significant color change. The palladium loading was estimated by inductively coupled plasma optical emission spectrometry (ICP-OES) to be  $\sim 40$  wt%, which is a very high loading. In reality, usually  $>20$  wt% of NPs loading leads to agglomeration of particles, as reported previously.<sup>13b</sup> Interestingly, transmission electron microscopy (TEM) of  $\text{Pd@}$

$\text{CCI}^{\text{f}}$  suggests well-dispersed PdNPs with a narrow size distribution, having a mean particle size of  $1.8 \pm 0.2$  nm (Figure 3). Based on this value, which matches well with the estimated

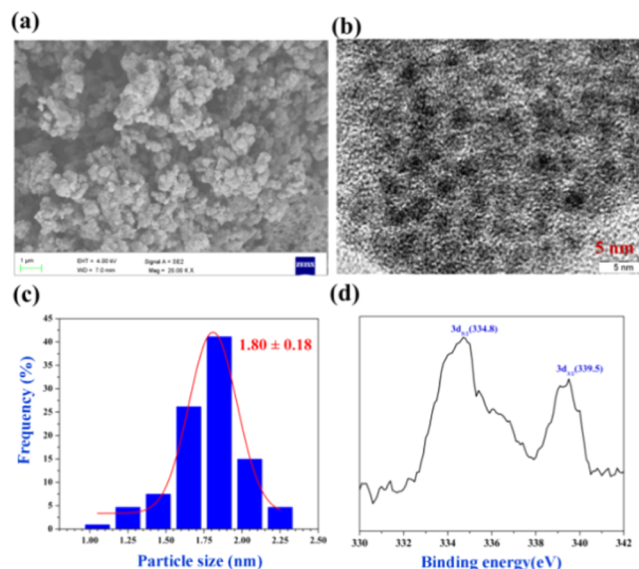


**Figure 3.** (a) SEM, (b) TEM, (c) particle size distribution, and (d) XPS spectra of  $\text{Pd@CCI}^{\text{f}}$ .

internal cavity size ( $\sim 2.0$  nm) of the cage, we believe that most of the NPs are probably anchored within the cage. The scanning electron microscopy (SEM) image portrays a rough morphology composed of granular particles (Figure 3). Powder X-ray diffraction (PXRD) analysis displayed peaks at  $2\theta \approx 40^\circ$ ,  $47^\circ$ ,  $68^\circ$ ,  $82^\circ$ , and  $87^\circ$  which could be ascribed respectively to (111), (200), (220), (311), and (222) lattice planes, a typical signature for Pd with a face-centered cubic (fcc) structure (Figure S24). Additionally X-ray photoelectron spectroscopy (XPS) suggests that Pd is in the zero oxidation state, as indicated by the characteristic binding energy values 334.8 and 339.5 eV, corresponding to two distinct spin–orbit pairs,  $3d_{5/2}$  and  $3d_{3/2}$ , respectively (Figure 3).

In order to understand the role of structural features (size and shape) of organic cages in the growth of NPs, we extended our synthetic strategy for the synthesis of  $\text{Pd@CC}2^{\text{f}}$ . However, unlike the previous case, herein we observed an immediate formation of greenish-yellow precipitate when  $\text{CC}2^{\text{f}}$  was treated with 12 equiv (corresponds to 12 diamine clefts) of  $\text{Pd}(\text{OAc})_2$  in  $\text{CHCl}_3$ . To obtain the desired material, the reaction mixture was treated with excess methanolic  $\text{NaBH}_4$ , which turned the color of the precipitate to black, indicating efficient reduction of  $\text{Pd}^{2+}$  into  $\text{Pd}^0$  (Figure S23). As-obtained black  $\text{Pd@CC}2^{\text{f}}$  was found to be insoluble in any common organic solvent, making it a perfect candidate for heterogeneous catalysis. This material was characterized in a similar manner by TEM, SEM, PXRD, XPS, and ICP-OES.

The ICP-OES estimated  $\sim 25$  wt% of palladium loading. In PXRD and XPS spectra, characteristic peaks corresponding to  $\text{Pd}^0$  NPs with fcc structure were observed (Figures S25 and S26). The TEM analysis indicated well-dispersed NPs with a mean size of  $3.7 \pm 0.4$  nm. The fact that the PdNPs have much larger sizes than the cage cavity ( $\sim 2.4$  nm) suggests that, in this case, most of the particles are anchored on the cage periphery, where a PdNP could be stabilized by multiple cages (Scheme S2), unlike what we observed in  $\text{Pd@CCI}^{\text{f}}$ . Such a marked difference in loading

and particle sizes of PdNPs with the change of cage compounds indicates the important role of structural features of the organic cage in NPs growth.

To further investigate the role of the cage scaffold in PdNP synthesis, we performed a controlled experiment. In that case, Pd(OAc)<sub>2</sub> in chloroform was treated with excess methanolic NaBH<sub>4</sub>, but in the absence of any of the cage compounds. TEM analysis of the obtained black precipitate (commonly known as palladium black) suggested the formation of structure-less agglomerates (Figure S27). Such agglomeration is undoubtedly due to the lack of nucleation (i.e., Pd binding) sites, which in turn advocates for the role of organic walls and diamine moieties of the cages in controlling PdNPs' size.

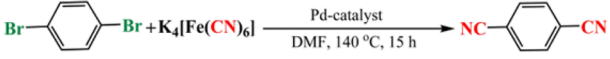
**Cyanation of Aryl Halides.** From the perspective of a synthetic organic chemist, cyanide is one of the most desirable functionalities, as it could easily be converted into several other functional moieties like aldehyde, ketone, carboxylic acid, amine, oxime, amidine, and so on. Moreover, aromatic nitriles are the key building blocks for many natural products and commercially available drugs, and they have been used extensively in agrochemical and dye industries.<sup>16</sup> The aromatic nitriles are commonly synthesized by the Sandmeyer and Rosenmund–von Braun reactions.<sup>17</sup> However, the major concern associated with these synthetic methodologies is associated with the use of elevated reaction temperatures (150–200 °C) and superstoichiometric amounts of toxic cyanating agent CuCN, which produces an equimolar amount of heavy metal wastes.

Recently, transition-metal-catalyzed cyanation has received wide attention.<sup>12e,18</sup> In this context, so far several transition metals, including Pd, Ni, and Cu, have been tested, among which Pd-catalyzed cyanation was found to be most beneficial, considering the milder reaction conditions and higher functional group tolerance.<sup>18a</sup> In order to address the safety concerns associated with the cyanide sources, nontoxic and inexpensive K<sub>4</sub>[Fe(CN)<sub>6</sub>] has been employed recently as cyanating agent.<sup>18b,e</sup> Since then, several palladium-based catalysts involving this reagent as a cyanide source have been developed. However, most of them employ expensive ligands and additives and suffer severely due to poor recyclability of the catalysts.<sup>18k</sup> Therefore, a more convenient and cost-effective synthetic protocol needs to be developed for this important chemical transformation.

To evaluate the catalytic activity of the cage-anchored PdNPs, transformation of 1,4-dibromobenzene to 1,4-dicyanobenzene has been selected as the model reaction. For the screening of the reaction parameters, a series of experiments was carried out with varying time, temperature, and catalyst loading. Reactions carried out employing Pd@CC1<sup>r</sup> as catalyst suggested that the best result (~99% product yield) could be obtained with 2 mol% Pd and 0.34 equiv of K<sub>4</sub>[Fe(CN)<sub>6</sub>] in DMF after heating the reaction mixtures at 140 °C under an inert atmosphere for 15 h (Table 1, entry 3). Variation in any one of the reaction parameters was found to have a profound effect on the yield of the desired product; e.g., when the reaction was carried out at 130 °C while keeping the other reaction parameters unaltered, we observed a sharp decrease in the yield (Table 1, entry 6).

It is a well-established fact that the catalytic activity of NPs greatly depends on their size, wherein an increase in size leads to a decrease in their catalytic activity. Therefore, a lower catalytic activity would be expected for Pd@CC2<sup>r</sup> than Pd@CC1<sup>r</sup>. To investigate this issue, the aforementioned reaction was carried out employing Pd@CC2<sup>r</sup> as catalyst. The results indicated that higher (4 mol% Pd) catalyst loading was required to achieve ~90% yield (which is lower than the yield obtained with Pd@

**Table 1. Standardization of Reaction Parameters for the Cyanation of 1,4-Dibromobenzene<sup>a</sup>**



entry	temp (°C)	time (h)	mol% Pd		yield (%)	
			Pd@CC1 <sup>r</sup>	Pd@CC2 <sup>r</sup>	Pd@CC1 <sup>r</sup>	Pd@CC2 <sup>r</sup>
1	140	15	1	2	46	76
2	140	15	1.5	3	77	84
3	140	15	2	4	99	90
4	140	15		4.5		90
5	140	20		4		98
6	130	15	2	4	76	65
7	140	14	2	4	98	80
8	140	12	2	4	75	68

<sup>a</sup>Reactions were carried out using 0.34 mmol of K<sub>4</sub>[Fe(CN)<sub>6</sub>]·3H<sub>2</sub>O.

CC1<sup>r</sup>) under the same reaction conditions (Table 2, entry 3). Furthermore, it was observed that, to achieve a comparable yield

**Table 2. Cyanation of 1,4-Dibromobenzene by Different Pd Catalysts<sup>a,b</sup>**

entry	Pd catalyst (4 mol%)	condition	yield (%)
1	Pd(PPh <sub>3</sub> ) <sub>4</sub>	homogeneous	26
2	Pd(PPh <sub>3</sub> ) <sub>2</sub> Cl <sub>2</sub>	homogeneous	40
3	Pd(OAc) <sub>2</sub>	homogeneous	45
4	PdCl <sub>2</sub>	homogeneous	4
5	Pd-black	heterogeneous	2
6	Pd@C	heterogeneous	46

<sup>a</sup>Reaction conditions: 1,4-dibromobenzene (1 mmol), K<sub>4</sub>[Fe(CN)<sub>6</sub>]·3H<sub>2</sub>O (0.34 mmol), 10 mL of DMF, 140 °C, 15 h. <sup>b</sup>Yields are based on <sup>1</sup>H NMR analysis of the crude product.

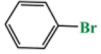
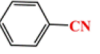
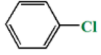
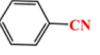
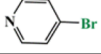
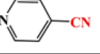
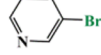
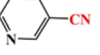
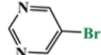
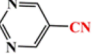
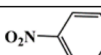
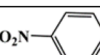
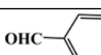
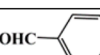
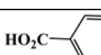
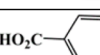
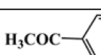
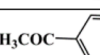
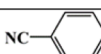
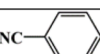
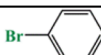
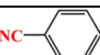
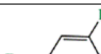

of the product as obtained with Pd@CC1<sup>r</sup> catalyst, a longer reaction time is required (Table 2, entry 5). These experimental results support the size-dependent catalytic activity of PdNPs in the present cases. Noticeably, when the model reaction was tested in the presence of several commonly used palladium catalysts under homogeneous/heterogeneous conditions, the yields of the desired product were much less.

To explore the generality of the catalytic systems, we extended our synthetic strategy for aryl halides bearing a wide variety of diverse functionalities to produce the corresponding nitriles. As shown in Table 3, we observed quantitative yields of nitriles in most cases. Most importantly, besides dibromobenzene, these catalytic systems have great potential to convert other aromatic polyhalides, like tribromobenzene, to the corresponding tricyanobenzene with reasonably good yield, which is generally hard to achieve under normal reaction conditions. Furthermore, less reactive chlorobenzene was cleanly converted to benzonitrile with quite high yields (Table 3, entry 2).

Reusability is the key issue for practical application of any heterogeneous catalyst, which makes it more beneficial over its homogeneous counterpart, particularly when precious metals are used. Therefore, to address this issue, the performance of both catalytic systems was tested for the model chemical transformation (1,4-dibromobenzene → 1,4-dicyanobenzene) up to five consecutive cycles. As portrayed in Figure 4, experimental results indicate a negligible decrease in their catalytic activity, while TEM images of the recovered materials after five cycles suggest no considerable change in the NPs' size and morphology

**Table 3.** Pd@CC1<sup>r</sup>/Pd@CC2<sup>r</sup>-Catalyzed Cyanation of Various Aryl Halides Using K<sub>4</sub>[Fe(CN)<sub>6</sub>]<sup>a,b</sup>

$$\text{Ar-X} + \text{K}_4[\text{Fe}(\text{CN})_6] \xrightarrow[\text{DMF, 140 }^\circ\text{C, 15 h}]{\text{Pd-catalyst}} \text{Ar-CN}$$

entry	aryl halide	product	yield [%]	
			Pd@CC1 <sup>r</sup>	Pd@CC2 <sup>r</sup>
1			99	99
2			97	94
3			99	97
4			98	96
5			>99	>99
6			>99	>99
7			>99	>99
8			>99	>99
9			97	90
10			99	94
11 <sup>c</sup>			99	90
12 <sup>d</sup>			92	51

<sup>a</sup>Reaction condition: aryl halides (1 mmol), K<sub>4</sub>[Fe(CN)<sub>6</sub>].3H<sub>2</sub>O (0.17 mmol), Pd@CC1<sup>r</sup> (5.3 mg, 2 mol% Pd)/Pd@CC2<sup>r</sup> (17 mg, 4 mol% Pd), 10 mL of DMF. <sup>b</sup>Yields are based on <sup>1</sup>H NMR analysis of the crude products. <sup>c</sup>0.34 mmol of K<sub>4</sub>[Fe(CN)<sub>6</sub>].3H<sub>2</sub>O was used. <sup>d</sup>0.51 mmol of K<sub>4</sub>[Fe(CN)<sub>6</sub>].3H<sub>2</sub>O was used.

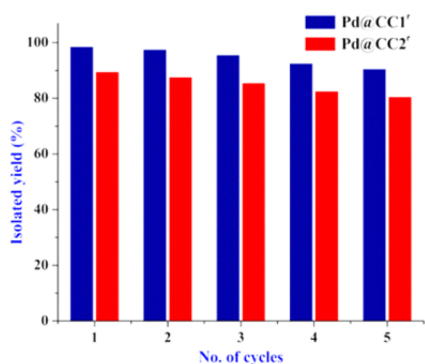


**Figure 4.** Recyclability of the Pd@cage catalysts.

(Figure S28). These results further support the fact that the ultrafine PdNPs are strongly bound to the cage, and such an interaction is stable even after prolonged heating of the material at high temperature.

## CONCLUSIONS

In summary, we have demonstrated that shape-persistent organic cage compounds having a porous interior and stable aromatic backbone with multiple diamine clefts foster the controlled synthesis of PdNPs. The strong binding affinity of Pd<sup>2+</sup> with the diamine clefts of the cage compounds is considered to be one of the governing factors during nucleation of the PdNPs, whereas aromatic walls protect the newly born NPs from agglomeration. The present results demonstrate the potential of functionalized discrete organic cage compounds as a novel platform for the size-controlled synthesis of PdNPs. Moreover, experimental results suggest that nanoparticles' size distribution and catalytic activity could be fine-tuned by changing the size of the cage compounds. It has been observed that PdNPs may anchor inside or outside the cage cavity, depending on the cage architecture. As-synthesized cage-anchored PdNPs were found to have better catalytic activity over several commercially available palladium catalysts, offering additive-free cyanation of haloarenes under heterogeneous conditions. The promising features of these catalysts include easy operational methodology, wide variety of functional group tolerance, reusability, and high yield of the products.

## EXPERIMENTAL SECTION

**Materials and Methods.** All the chemicals and solvents were purchased from commercially available sources and were used without further purification. The NMR spectra were recorded on Bruker 400 MHz instrument. The chemical shifts ( $\delta$ ) in the <sup>1</sup>H NMR spectra are recorded in ppm relative to tetramethylsilane (Me<sub>4</sub>Si) as an internal standard (0.0 ppm) in CDCl<sub>3</sub> or proton resonance resulting from incomplete deuteration of the solvents. High-resolution mass spectra were recorded on a Q-TOF instrument by electrospray ionization using standard spectroscopic-grade solvents. IR spectra were recorded on a Bruker ALPHA FTIR spectrometer. PXRD patterns were recorded on a Phillips PANalytical diffractometer. Scanning electron microscopy was performed on a Carl-Zeiss Ultra 55 instrument at an operating voltage of 5–20 kV. Transmission electron microscopy was performed on a JEOL 2100F instrument operating at 200 kV. X-ray photoelectron spectroscopy was carried out on an Axis Ultra instrument. Inductively coupled plasma optical emission spectrometry was carried out on a Thermo-iCAP 6000 Series instrument.

**Synthesis of Aldehyde C.** In a 100 mL flame-dried double-neck round-bottom flask, 0.96 g (2.00 mmol) of tris(4-bromophenyl)amine (A) and 1.40 g (9.33 mmol) of 3-formylphenylboronic acid (B) were taken in 50 mL of THF, and into that was added 20 mL of an aqueous solution of 1.40 g (10.00 mmol) of K<sub>2</sub>CO<sub>3</sub>. The resulting mixture was stirred under nitrogen atmosphere at room temperature for 10 min, followed by addition of 0.12 g (0.10 mmol) of Pd(PPh<sub>3</sub>)<sub>4</sub>, and heated to 75 °C for 48 h. After completion of the reaction, THF was removed, and the aqueous part was extracted with dichloromethane (50 mL × 3). The organic part was then dried over Na<sub>2</sub>SO<sub>4</sub> and completely removed to obtain a pale yellow solid. The resulting solid mass was purified by silica gel column chromatography in dichloromethane to get a greenish yellow powder. Isolated yield: 58% (0.65 g, 1.16 mmol). Single crystals of the compound were obtained from a CHCl<sub>3</sub>-EtOAc solution by slow evaporation. <sup>1</sup>H NMR (CDCl<sub>3</sub>, 400 MHz):  $\delta$  10.09 (s, 3H), 8.11 (s, 3H), 7.83–7.88 (m, 6H), 7.57–7.63 (m, 9H), 7.28 (d, 6H). <sup>13</sup>C NMR (100 MHz, CDCl<sub>3</sub>):  $\delta$  192.8, 147.7, 141.9, 137.4, 134.9, 133.0, 130.0, 128.9, 128.6, 128.1, 125.1. ESI-HRMS (CHCl<sub>3</sub>-CH<sub>3</sub>CN): *m/z* for C<sub>39</sub>H<sub>27</sub>NO<sub>3</sub>, [M]<sup>+</sup> 557.1981 (calcd 557.1990). FTIR (cm<sup>-1</sup>):  $\nu$  1691 (CH=O), 1594, 1510, 1471, 1438, 1386, 1296, 1283, 1263, 1179, 1160, 900, 842, 829, 783, 738, 686, 641, 563, 531.

**Synthesis of CC1.** In a 250 mL round-bottom flask, 120 mL of a CHCl<sub>3</sub> solution of diamine D (31 mg, 0.28 mmol) was added slowly, dropwise, to a stirring solution of aldehyde C (100 mg, 0.18 mmol) dissolved in 60 mL of CHCl<sub>3</sub>. The resulting reaction mixture was heated to reflux for 48 h. After completion of the reaction, solvent was removed,

and the obtained pale yellow solid was washed with CH<sub>3</sub>CN several times. Isolated yield: 91% (110 mg, 0.08 mmol). <sup>1</sup>H NMR (CDCl<sub>3</sub>, 400 MHz): δ 8.37 (s, 6H), 7.86 (s, 6H), 7.55 (d, 12H), 7.36–7.40 (m, 18H), 7.10 (d, 12H), 3.44 (d, 6H), 1.88–1.95 (m, 18H), 1.51 (m, 6H). <sup>13</sup>C NMR (100 MHz, CDCl<sub>3</sub>): δ 162.0, 147.4, 141.4, 137.5, 135.6, 129.4, 129.0, 128.4, 126.8, 126.7, 125.1, 74.1, 33.3, 25.0. ESI-HRMS (CHCl<sub>3</sub>–CH<sub>3</sub>CN): *m/z* for C<sub>96</sub>H<sub>84</sub>N<sub>8</sub>, [M+H]<sup>+</sup> 1350.6999 (calcd 1350.6931), [M+2H]<sup>2+</sup> 675.8494 (calcd 675.8818). FTIR (cm<sup>-1</sup>): ν 2929, 2851, 1646 (CH=N), 1600, 1516, 1477, 1471, 1315, 1276, 1250, 1084, 1010, 829, 790, 686, 538.

**Synthesis of CC1'.** In a 100 mL round-bottom flask, 100 mg (0.07 mmol) of CC1 was taken in 60 mL of a CHCl<sub>3</sub>–MeOH (1:1, v/v) binary solvent mixture. Into this reaction mixture was added 32 mg (0.84 mmol) of NaBH<sub>4</sub> portionwise at room temperature, followed by stirring for 12 h. After completion of the reaction, solvent was completely removed, and the product was extracted in CHCl<sub>3</sub>. The organic part was washed several times with water and dried over Na<sub>2</sub>SO<sub>4</sub>, followed by removal of solvent to get a white solid. Isolated yield: 85% (81 mg, 0.06 mmol). <sup>1</sup>H NMR (CDCl<sub>3</sub>, 400 MHz): δ 7.57 (s, 6H), 7.33–7.39 (m, 12H), 7.19–7.25 (m, 18H), 6.92 (d, 12H), 3.94 (d, 6H), 3.62 (d, 6H), 2.31 (br m, 18H), 1.78 (br s, 12H), 1.27–1.32 (br m, 6H), 1.08 (br s, 6H). <sup>13</sup>C NMR (100 MHz, CDCl<sub>3</sub>): δ 146.9, 141.7, 141.6, 135.8, 129.2, 128.1, 127.8, 127.0, 125.9, 124.9, 61.7, 51.8, 32.0, 25.6. ESI-HRMS (CHCl<sub>3</sub>–CH<sub>3</sub>CN): *m/z* for C<sub>96</sub>H<sub>96</sub>N<sub>8</sub>, [M+H]<sup>+</sup> 1361.7697 (calcd 1361.7836), [M+2H]<sup>2+</sup> 681.3862 (calcd 681.3957). FTIR (cm<sup>-1</sup>): ν 2929, 2844, 2358, 1600, 1510, 1471, 1438, 1321, 1283, 1101, 835, 790, 738, 693.

**Synthesis of CC2.** This cage was synthesized following the same synthetic protocol employed for CC1, from tris(4-formylphenyl)amine (100 mg, 0.30 mmol) and D (50 mg, 0.45 mmol). Isolated yield: 80% (107 mg, 0.03 mmol). <sup>1</sup>H NMR (CDCl<sub>3</sub>, 400 MHz): δ 8.35 (s, 12H), 8.24 (s, 12H), 7.61–7.55 (m, 48H), 7.08–7.02 (m, 48H), 3.56–3.48 (m, 24H), 1.85 (br, 24H), 1.75 (br, 48H), 1.49 (br, 24H). ESI-HRMS (CHCl<sub>3</sub>–MeOH): *m/z* for C<sub>240</sub>H<sub>240</sub>N<sub>32</sub>, [M+2H]<sup>2+</sup> 1787.0146 (calcd 1786.9995), [M+3H]<sup>3+</sup> 1191.9636 (calcd 1191.9039).

**Synthesis of CC2'.** In a 100 mL round-bottom flask, 71 mg (0.02 mmol) of CC2 was taken in 60 mL of a CHCl<sub>3</sub>–MeOH (1:1, v/v) binary solvent mixture. To this reaction mixture was added 38 mg (1 mmol) of NaBH<sub>4</sub> portionwise at room temperature, followed by stirring for 12 h. After completion of the reaction, solvent was completely removed, and the product was extracted in CHCl<sub>3</sub>. The organic part was washed several times with water and dried over sodium sulfate, followed by removal of solvent to get a yellow solid. Isolated yield: 77% (39 mg, 0.015 mmol). <sup>1</sup>H NMR (CDCl<sub>3</sub>, 400 MHz): δ 7.08 (d, 48H), 6.89 (d, 48H), 3.76 (d, 24H), 3.52 (d, 24H), 2.1–2.26 (br m, 72H), 1.7 (br d, 24H), 1.15–1.27 (br m, 24H). ESI-HRMS (CHCl<sub>3</sub>–MeOH): *m/z* for C<sub>240</sub>H<sub>288</sub>N<sub>32</sub>, [M+2H]<sup>2+</sup> 1809.4375 (calcd 1809.4406), [M+3H]<sup>3+</sup> 1206.7337 (calcd 1206.6763).

**Synthesis of Pd@CC1' Catalyst.** In a typical synthetic protocol, 40 mg (0.03 mmol) of CC1' dissolved in 6 mL of CHCl<sub>3</sub> was treated with 4 mL of a CHCl<sub>3</sub> solution of 20 mg (0.09 mmol) of Pd(OAc)<sub>2</sub> for 1 h. Into this reaction mixture was added a methanolic solution of NaBH<sub>4</sub> (24.3 mg, 0.18 mmol) dropwise at room temperature, followed by stirring for 20 min. After the reported time period, the solvent was completely removed, and the product was washed several times with methanol, followed by drying under vacuum overnight to obtain Pd@CC1' as a black solid.

**Synthesis of Pd@CC2' Catalyst.** In a typical synthetic protocol, 40 mg (0.01 mmol) of CC2' dissolved in 8 mL of CHCl<sub>3</sub> was treated with 4 mL of a CHCl<sub>3</sub> solution of 29.0 mg (0.12 mmol) of Pd(OAc)<sub>2</sub> for 2 h. Into this reaction mixture was added a methanolic solution of NaBH<sub>4</sub> (36.6 mg, 0.26 mmol) dropwise at room temperature, followed by stirring for 40 min. After the reported time period, the precipitated black solid was filtered out and washed several times with methanol, followed by drying under vacuum overnight to obtain the desired catalyst Pd@CC2'.

**Sample Preparation for ICP-OES Analysis.** In a typical stock solution preparation, 7 mg of Pd@cage was added to 10 mL of concentrated nitric acid and stirred overnight at room temperature. After complete dissolution of the compound, the solution was filtered to

remove any undissolved material. The filtrate was then diluted with deionized water to make a 100 mL stock solution.

**General Experimental Procedure for Cyanation of Aryl Halides.** A representative procedure for the cyanation of 1,4-dibromobenzene with K<sub>4</sub>[Fe(CN)<sub>6</sub>] is described here. In a flame-dried 50 mL round-bottom flask, 236 mg (1.00 mmol) of 1,4-dibromobenzene, 73 mg (0.17 mmol) of K<sub>4</sub>[Fe(CN)<sub>6</sub>]·3H<sub>2</sub>O, and 5.3 mg (0.02 mmol PdNPs) of Pd@CC1' or 17 mg (0.04 mmol PdNPs) of Pd@CC2' were taken in 10 mL of DMF. The resulting reaction mixture was stirred under nitrogen atmosphere at 140 °C for 15 h. After completion of the reaction, the mixture was filtered to separate the solid catalyst. The filtrate was then extracted with EtOAc (3 × 10 mL). The organic part was washed with water and dried over Na<sub>2</sub>SO<sub>4</sub>, followed by complete removal of solvent. The resulting solid mass was purified by silica gel column chromatography in hexane/dichloromethane (1:9 v/v) to afford pure 1,4-dicyanobenzene as a white solid. <sup>1</sup>H NMR (CDCl<sub>3</sub>, 400 MHz): δ 7.79 (s, 4H). <sup>13</sup>C NMR (100 MHz, CDCl<sub>3</sub>): δ 133.3, 117.5, 117.2.

**4-Pyridinecarbonitrile.** <sup>1</sup>H NMR (CDCl<sub>3</sub>, 400 MHz): δ 8.76 (d, 2H), 7.49 (d, 2H). <sup>13</sup>C NMR (100 MHz, CDCl<sub>3</sub>): δ 151.2, 125.7, 120.8, 116.8.

**3-Pyridinecarbonitrile.** <sup>1</sup>H NMR (CDCl<sub>3</sub>, 400 MHz): δ 8.83 (s, 1H), 8.75–8.77 (m, 1H), 7.91–7.94 (m, 1H), 7.39–7.42 (m, 1H). <sup>13</sup>C NMR (100 MHz, CDCl<sub>3</sub>): δ 153.5, 152.9, 139.7, 124.1, 117.0, 110.5.

**4-Formylbenzonitrile.** <sup>1</sup>H NMR (CDCl<sub>3</sub>, 400 MHz): δ 10.06 (s, 1H), 7.96 (d, 2H), 7.81 (d, 2H). <sup>13</sup>C NMR (100 MHz, CDCl<sub>3</sub>): δ 191.3, 139.2, 133.4, 130.4, 118.0.

**4-Cyanobenzoic Acid.** <sup>1</sup>H NMR (CD<sub>3</sub>OD, 400 MHz): δ 8.15 (d, 2H), 7.84 (d, 2H). <sup>13</sup>C NMR (100 MHz, CD<sub>3</sub>OD): δ 167.4, 135.9, 132.4, 130.3, 118.1, 116.0.

**Benzonitrile.** <sup>1</sup>H NMR (CDCl<sub>3</sub>, 400 MHz): δ 7.58–7.63 (m, 3H), 7.45–7.48 (m, 2H). <sup>13</sup>C NMR (100 MHz, CDCl<sub>3</sub>): δ 133.4, 132.6, 129.8, 119.4, 112.8.

**4-Nitrobenzonitrile.** <sup>1</sup>H NMR (CDCl<sub>3</sub>, 400 MHz): δ 8.35 (d, 2H), 7.89 (d, 2H). <sup>13</sup>C NMR (100 MHz, CDCl<sub>3</sub>): δ 150.4, 134.0, 124.8, 118.8, 117.3.

**4-Acetylbenzonitrile.** <sup>1</sup>H NMR (CDCl<sub>3</sub>, 400 MHz): δ 8.03 (d, 2H), 7.77 (d, 2H), 2.64 (s, 3H). <sup>13</sup>C NMR (100 MHz, CDCl<sub>3</sub>): δ 196.6, 140.0, 132.6, 128.8, 118.0, 116.5, 26.8.

**5-Cyanopyrimidine.** <sup>1</sup>H NMR (CDCl<sub>3</sub>, 400 MHz): δ 9.4 (s, 1H), 9.0 (s, 2H). <sup>13</sup>C NMR (100 MHz, CDCl<sub>3</sub>): δ 160.8, 159.7, 114.3, 110.5.

**1,3,5-Tricyanobenzene.** <sup>1</sup>H NMR (CDCl<sub>3</sub>, 400 MHz): δ 8.17 (s, 3H). <sup>13</sup>C NMR (100 MHz, DMSO-*d*<sub>6</sub>): δ 141.2, 116.7, 114.9.

**Computational Methodology.** Full geometry optimizations were performed using the Gaussian 09 package.<sup>19</sup> The hybrid B3LYP functional was used in all calculations as implemented in the Gaussian 09 package, mixing the exact Hartree–Fock-type exchange with Becke's expression for the exchange functional<sup>20</sup> that was proposed by Lee, Yang, and Parr for the correlation contribution.<sup>21</sup> The 6-31G basis set was used for all calculations. Frequency calculations carried out on the optimized structures confirmed the absence of any imaginary frequencies.

**X-ray Crystal Data Collection and Structure Solution.** X-ray data of the aldehyde C were collected on a Bruker D8 QUEST CMOS diffractometer using the SMART/SAINT<sup>22</sup> software, equipped with a low-temperature device. The diffraction-quality crystal was mounted on a loop coated with traces of viscous oil. The intensity data were collected at 100(2) K using graphite-monochromated Mo K $\alpha$  radiation (0.7107 Å). The structure was solved by direct methods and refined by full matrix least-squares on *F*<sup>2</sup>, employing SHELX-97<sup>23</sup> incorporated in WinGX.<sup>24</sup> Empirical absorption corrections were applied with SADABS.<sup>25</sup> All non-hydrogen atoms were refined anisotropically. Hydrogen atoms were placed by using the riding models and refined isotropically. Crystallographic data and refinement parameters are provided in Table S1 and the supporting CIF file.

## ■ ASSOCIATED CONTENT

## ■ Supporting Information

The Supporting Information is available free of charge on the ACS Publications website at DOI: 10.1021/jacs.5b13307.

Syntheses and characterization data (NMR, FTIR, ESI-MS, TEM, SEM, PXRD), including Figures S1–S48, Table S1, and Schemes S1 and S2 (PDF)

X-ray crystallographic data for C (CIF)

## ■ AUTHOR INFORMATION

## Corresponding Author

\*psm@ipc.iisc.ernet.in

## Author Contributions

‡B.M. and K.A. contributed equally.

## Notes

The authors declare no competing financial interest.

## ■ ACKNOWLEDGMENTS

P.S.M. is grateful to DST-New Delhi (India) for financial support. B.M. gratefully acknowledges the CSIR, New Delhi, for the award of a research fellowship. We are thankful to Mr. Imtiyaz Ahmad Bhat for mass spectral analysis and Mr. Sourav Ghosh for powder XRD data collection and TEM analysis.

## ■ REFERENCES

- (1) (a) Wang, M.; Vajpayee, V.; Shanmugaraju, S.; Zheng, Y.; Zhao, Z.; Kim, H.; Mukherjee, P. S.; Chi, K.-W.; Stang, P. J. *Inorg. Chem.* **2011**, *50*, 1506. (b) Dong, J.; Zhou, Y.; Zhang, F.; Cui, Y. *Chem. - Eur. J.* **2014**, *20*, 6455. (c) Xuan, W.; Zhang, M.; Liu, Y.; Chen, Z.; Cui, Y. *J. Am. Chem. Soc.* **2012**, *134*, 6904. (d) Zhang, J.; Li, Y.; Yang, W.; Lai, S.; Zhou, C.; Liu, H.; Che, C.; Li, Y. *Chem. Commun.* **2012**, *48*, 3602.
- (2) (a) Murase, T.; Nishijima, Y.; Fujita, M. *J. Am. Chem. Soc.* **2012**, *134*, 162. (b) Zhao, C.; Sun, Q.; Hart-Cooper, W. M.; DiPasquale, A. G.; Toste, F. D.; Bergman, R. G.; Raymond, K. N. *J. Am. Chem. Soc.* **2013**, *135*, 18802. (c) Zhang, Q.; Tiefenbacher, K. *J. Am. Chem. Soc.* **2013**, *135*, 16213. (d) Hart-Cooper, W. M.; Clary, K. N.; Toste, F. D.; Bergman, R. G.; Raymond, K. N. *J. Am. Chem. Soc.* **2012**, *134*, 17873.
- (3) (a) Tiefenbacher, K.; Rebek, J. *J. Am. Chem. Soc.* **2012**, *134*, 2914. (b) Jiang, W.; Rebek, J. *J. Am. Chem. Soc.* **2012**, *134*, 17498. (c) Roy, B.; Ghosh, A. K.; Srivastava, S.; D'Silva, P.; Mukherjee, P. S. *J. Am. Chem. Soc.* **2015**, *137*, 11916. (d) Zhang, K.; Ajami, D.; Gavette, J. V.; Rebek, J. *J. Am. Chem. Soc.* **2014**, *136*, 5264. (e) Yang, Y.; Chen, J.; Liu, J.; Zhao, G.; Liu, L.; Han, K.; Cook, T. R.; Stang, P. J. *J. Phys. Chem. Lett.* **2015**, *6*, 1942. (f) Zheng, Y.; Zhao, Z.; Kim, H.; Wang, M.; Ghosh, K.; Pollock, J. B.; Chi, K.-W.; Stang, P. J. *Inorg. Chem.* **2010**, *49*, 10238. (g) Huang, S.-L.; Lin, Y.-J.; Hor, T. S. A.; Jin, G.-X. *J. Am. Chem. Soc.* **2013**, *135*, 8125. (h) Han, Y.-F.; Lin, Y.-J.; Hor, T. S. A.; Jin, G.-X. *Organometallics* **2012**, *31*, 995.
- (4) (a) Sun, Q. F.; Sato, S.; Fujita, M. *Nat. Chem.* **2012**, *4*, 330. (b) Suzuki, K.; Tominaga, M.; Kawano, M.; Fujita, M. *Chem. Commun.* **2009**, 1638. (c) Hong, M.; Zhao, Y.; Su, W.; Cao, R.; Fujita, M.; Zhou, Z.; Chan, A. S. C. *J. Am. Chem. Soc.* **2000**, *122*, 4819. (d) Ronson, T. K.; Fisher, J.; Harding, L. P.; Rizkallah, P. J.; Warren, J. E.; Hardie, M. J. *Nat. Chem.* **2009**, *1*, 212. (e) Duriska, M. B.; Neville, S. M.; Lu, J.; Iremonger, S. S.; Boas, J. F.; Kepert, C. J.; Batten, S. R. *Angew. Chem., Int. Ed.* **2009**, *48*, 8919. (f) Duriska, M. B.; Neville, S. M.; Moubaraki, B.; Cashion, J. D.; Halder, G. J.; Chapman, K. W.; Balde, C.; Letard, J.; Murray, K. S.; Kepert, C. J.; Batten, S. R. *Angew. Chem., Int. Ed.* **2009**, *48*, 2549. (g) Moon, D.; Kang, S.; Park, J.; Lee, K.; John, R. P.; Won, H.; Seong, G. H.; Kim, Y. S.; Kim, G. H.; Rhee, H.; Lah, M. S. *J. Am. Chem. Soc.* **2006**, *128*, 3530. (h) Bhat, I. A.; Samanta, D.; Mukherjee, P. S. *J. Am. Chem. Soc.* **2015**, *137*, 9497. (i) Samanta, D.; Mukherjee, P. S. *J. Am. Chem. Soc.* **2014**, *136*, 17006. (j) Bar, A. K.; Chakrabarty, R.; Mostafa, G.; Mukherjee, P. S. *Angew. Chem., Int. Ed.* **2008**, *47*, 8455. (k) Chakrabarty, R.; Mukherjee, P. S.; Stang, P. J. *Chem. Rev.* **2011**, *111*, 6810.

- (l) Mukherjee, S.; Mukherjee, P. S. *Chem. Commun.* **2014**, *50*, 2239. (m) Granzhan, A.; Schouwey, C.; Riis-Johannessen, T.; Scopelliti, R.; Severin, K. *J. Am. Chem. Soc.* **2011**, *133*, 7106. (n) Smulders, M. M. J.; Jiménez, A.; Nitschke, J. R. *Angew. Chem., Int. Ed.* **2012**, *51*, 6681. (o) Sarma, R. J.; Nitschke, J. R. *Angew. Chem., Int. Ed.* **2008**, *47*, 377.
- (5) (a) Ye, Y.; Cook, T. R.; Wang, S. P.; Wu, J.; Li, S.; Stang, P. J. *J. Am. Chem. Soc.* **2015**, *137*, 11896. (b) Zheng, Y. R.; Lan, W. J.; Wang, M.; Cook, T. R.; Stang, P. J. *J. Am. Chem. Soc.* **2011**, *133*, 17045. (c) Wang, M.; Zheng, Y. R.; Ghosh, K.; Stang, P. J. *J. Am. Chem. Soc.* **2010**, *132*, 6282. (d) Fan, J.; Saha, M. L.; Song, B.; Schönherr, H.; Schmittel, M. *J. Am. Chem. Soc.* **2012**, *134*, 150. (e) Schmittel, M.; He, B.; Mal, P. *Org. Lett.* **2008**, *10*, 2513. (f) Sun, B.; Wang, M.; Lou, Z.; Huang, M.; Xu, C.; Li, X.; Chen, L. J.; Yu, Y.; Davis, G. L.; Xu, B.; Yang, H. B.; Li, X. *J. Am. Chem. Soc.* **2015**, *137*, 1556. (g) Xu, L.; Wang, Y.-X.; Chen, L.-J.; Yang, H.-B. *Chem. Soc. Rev.* **2015**, *44*, 2148. (h) Cook, T. R.; Stang, P. J. *Chem. Rev.* **2015**, *115*, 7001. (i) Jie, K.; Zhou, Y.; Yao, Y.; Shi, B.; Huang, F. *J. Am. Chem. Soc.* **2015**, *137*, 10472. (j) Li, Z.; Yang, J.; Yu, G.; He, J.; Abliz, Z.; Huang, F. *Org. Lett.* **2014**, *16*, 2066. (k) Lee, H.; Elumalai, P.; Singh, N.; Kim, H.; Lee, S. U.; Chi, K.-W. *J. Am. Chem. Soc.* **2015**, *137*, 4674. (l) Li, S.; Huang, J.; Cook, T. R.; Pollock, J. B.; Kim, H.; Chi, K.-W.; Stang, P. J. *J. Am. Chem. Soc.* **2013**, *135*, 2084. (m) Gianneschi, N. C.; Masar, M. S.; Mirkin, C. A. *Acc. Chem. Res.* **2005**, *38*, 825.
- (6) (a) Coughon, F. B. L.; Sanders, J. K. M. *Acc. Chem. Res.* **2012**, *45*, 2211. (b) Rowan, S. J.; Cantrill, S. J.; Cousins, G. R. L.; Sanders, J. K. M.; Stoddart, J. F. *Angew. Chem., Int. Ed.* **2002**, *41*, 898. (c) Reek, J. N. H.; Otto, S. *Dynamic Combinatorial Chemistry*; Wiley-VCH: Weinheim, 2010. (d) Lehn, J. M. *Chem. - Eur. J.* **1999**, *5*, 2455.
- (7) (a) Francesconi, O.; Ienco, A.; Moneti, G.; Nativi, C.; Roelens, S. *Angew. Chem., Int. Ed.* **2006**, *45*, 6693. (b) Mateus, P.; Delgado, R.; Brandão, P.; Félix, V. *J. Org. Chem.* **2012**, *77*, 4611. (c) Perraud, O.; Sorokin, A. B.; Dutasta, J. P.; Martinez, A. *Chem. Commun.* **2013**, *49*, 1288. (d) Mastalerz, M.; Schneider, W.; Oettel, I. M.; Presly, O. *Angew. Chem., Int. Ed.* **2011**, *50*, 1046. (e) Mitra, T.; Jelfs, K. E.; Schmidtman, M.; Ahmed, A.; Chong, S. Y. D.; Adams, J.; Cooper, A. I. *Nat. Chem.* **2013**, *5*, 276. (f) Brutschy, M.; Schneider, M. W.; Mastalerz, M.; Waldvogel, S. R. *Adv. Mater.* **2012**, *24*, 6049. (g) Jiang, S.; Jelfs, K. E.; Holden, D.; Hasell, T.; Chong, S. Y.; Haranczyk, M.; Trewin, A.; Cooper, A. I. *J. Am. Chem. Soc.* **2013**, *135*, 17818. (h) Skowronek, P.; Warzajtis, B.; Rychlewska, U.; Gawroński, J. *Chem. Commun.* **2013**, *49*, 2524. (i) Zhang, G.; Presly, O.; White, F.; Oettel, I. M.; Mastalerz, M. *Angew. Chem., Int. Ed.* **2014**, *53*, 5126. (j) Ding, H.; Yang, Y.; Li, B.; Pan, F.; Zhu, G.; Zeller, M.; Yuan, D.; Wang, C. *Chem. Commun.* **2015**, *51*, 1976. (k) Jin, Y.; Voss, B. A.; Jin, A.; Long, H.; Noble, R. D.; Zhang, W. *J. Am. Chem. Soc.* **2011**, *133*, 6650. (l) Acharyya, K.; Mukherjee, P. S. *Chem. - Eur. J.* **2015**, *21*, 6823. (m) Acharyya, K.; Mukherjee, P. S. *Chem. Commun.* **2014**, *50*, 15788. (n) Mastalerz, M. *Angew. Chem., Int. Ed.* **2010**, *49*, 5042.
- (8) (a) Acharyya, K.; Mukherjee, S.; Mukherjee, P. S. *J. Am. Chem. Soc.* **2013**, *135*, 554. (b) Acharyya, K.; Mukherjee, P. S. *Chem. - Eur. J.* **2014**, *20*, 1646. (c) Acharyya, K.; Mukherjee, P. S. *Chem. Commun.* **2015**, *51*, 4241.
- (9) (a) Sun, J. K.; Zhan, W. W.; Akita, T.; Xu, Q. *J. Am. Chem. Soc.* **2015**, *137*, 7063. (b) McCaffrey, R.; Long, H.; Jin, Y.; Sanders, A.; Park, W.; Zhang, W. *J. Am. Chem. Soc.* **2014**, *136*, 1782.
- (10) (a) Vajda, S.; Pellin, M. J.; Greeley, J. P.; Marshall, C. L.; Curtiss, L. A.; Ballentine, G. A.; Elam, J. W.; Catillon-Mucherie, S.; Redfern, P. C.; Mehmood, F. *Nat. Mater.* **2009**, *8*, 213. (b) Qiao, B.; Wang, A.; Yang, X.; Allard, L. F.; Jiang, Z.; Cui, Y.; Liu, J.; Li, J.; Zhang, T. *Nat. Chem.* **2011**, *3*, 634. (c) Li, Z.; Liu, J.; Xia, C.; Li, F. *ACS Catal.* **2013**, *3*, 2440. (d) Kibata, T.; Mitsudome, T.; Mizugaki, T.; Jitsukawa, K.; Kaneda, K. *Chem. Commun.* **2013**, *49*, 167. (e) Huang, W.; Liu, J. H.; Alayoglu, P.; Li, Y.; Witham, C. A.; Tsung, C. K.; Toste, F. D.; Somorjai, G. A. *J. Am. Chem. Soc.* **2010**, *132*, 16771. (f) Joo, S. H.; Park, J. Y.; Renzas, J. R.; Butcher, D. R.; Huang, W.; Somorjai, G. A. *Nano Lett.* **2010**, *10*, 2709.
- (11) (a) White, R. J.; Luque, R.; Budarin, V. L.; Clark, J. H.; Macquarrie, D. J. *Chem. Soc. Rev.* **2009**, *38*, 481.
- (12) (a) Nasir Baig, R. B. N.; Varma, R. S. *ACS Sustainable Chem. Eng.* **2013**, *1*, 805. (b) Chaudhury, A.; Gragnaniello, L.; Ma, T.; Surnev, S.; Netzer, F. P. *J. Phys. Chem. C* **2013**, *117*, 18112. (c) Balint, I.; Miyazaki,

- A.; Aika, K. *Chem. Commun.* **2002**, 630. (d) Prieto, G.; Zecevi, J.; Friedrich, H.; de Jong, K. P.; de Jongh, P. E. *Nat. Mater.* **2013**, *12*, 34. (e) Chatterjee, T.; Dey, R.; Ranu, B. C. *J. Org. Chem.* **2014**, *79*, 5875. (f) Campbell, C. T.; Starr, D. E. *J. Am. Chem. Soc.* **2002**, *124*, 9212. (g) Farmer, J. A.; Campbell, C. T. *Science* **2010**, *329*, 933. (h) Campbell, C. T. *Acc. Chem. Res.* **2013**, *46*, 1712.
- (13) (a) Aijaz, A.; Karkamkar, A.; Choi, Y. J.; Tsumori, N.; Rönnebro, E.; Autrey, T.; Shioyama, H.; Xu, Q. *J. Am. Chem. Soc.* **2012**, *134*, 13926. (b) Meilikhov, M.; Yusenko, K.; Esken, D.; Turner, S.; Tendeloo, G. V.; Fischer, R. A. *Eur. J. Inorg. Chem.* **2010**, *2010*, 3701. (c) Aijaz, A.; Xu, Q. *J. Phys. Chem. Lett.* **2014**, *5*, 1400. (d) Hermes, S.; Schröter, M. K.; Schmid, R.; Khodeir, L.; Muhler, M.; Tissler, A.; Fischer, R. W.; Fischer, R. A. *Angew. Chem., Int. Ed.* **2005**, *44*, 6237. (e) Ishida, T.; Nagaoka, M.; Akita, T.; Haruta, M. *Chem. - Eur. J.* **2008**, *14*, 8456. (f) Jiang, H. L.; Lin, Q. P.; Akita, T.; Liu, B.; Ohashi, H.; Oji, H.; Honma, T.; Takei, T.; Haruta, M.; Xu, Q. *Chem. - Eur. J.* **2011**, *17*, 78. (g) Esken, D.; Turner, S.; Lebedev, O. I.; Tendeloo, G. V.; Fischer, R. A. *Chem. Mater.* **2010**, *22*, 6393. (h) Jiang, H. L.; Liu, B.; Akita, T.; Haruta, M.; Sakurai, H.; Xu, Q. *J. Am. Chem. Soc.* **2009**, *131*, 11302. (i) Gole, B.; Sanyal, U.; Mukherjee, P. S. *Chem. Commun.* **2015**, *51*, 4872. (j) Hu, P.; Zhuang, J.; Chou, L.-Y.; Lee, H. K.; Ling, X. Y.; Chuang, Y.-C.; Tsung, C.-K. *J. Am. Chem. Soc.* **2014**, *136*, 10561. (k) Lu, G.; Li, S.; Guo, Z.; Farha, O. K.; Hauser, B. G.; Qi, X.; Wang, Y.; Wang, X.; Han, S.; Liu, X.; DuChene, J. S.; Zhang, H.; Zhang, Q.; Chen, X.; Ma, J.; Loo, S. C. J.; Wei, W. D.; Yang, Y.; Hupp, J. T.; Huo, F. *Nat. Chem.* **2012**, *4*, 310.
- (14) (a) Li, L.; Zhao, H.; Wang, J.; Wang, R. *ACS Nano* **2014**, *8*, 5352. (b) Zhang, P.; Weng, Z.; Guo, J.; Wang, C. *Chem. Mater.* **2011**, *23*, 5243. (c) Ding, S. Y.; Gao, J.; Wang, Q.; Zhang, Y.; Song, W. G.; Su, C. Y.; Wang, W. *J. Am. Chem. Soc.* **2011**, *133*, 19816. (d) Hasell, T.; Wood, C. D.; Clowes, R.; Jones, J. T. A.; Khimyak, Y. Z.; Adams, D. J.; Cooper, A. I. *Chem. Mater.* **2010**, *22*, 557. (e) Zhang, Q.; Yang, Y.; Zhang, S. *Chem. - Eur. J.* **2013**, *19*, 10024. (f) Chan-Thaw, C. E.; Villa, A.; Prati, L.; Thomas, A. *Chem. - Eur. J.* **2011**, *17*, 1052. (g) Zhou, Y.; Xiang, Z.; Cao, D.; Liu, C. *Chem. Commun.* **2013**, *49*, 5633. (h) Chan-Thaw, C. E.; Villa, A.; Katekomol, P.; Su, D.; Thomas, A.; Prati, L. *Nano Lett.* **2010**, *10*, 537. (i) Xie, Z.; Wang, C.; deKrafft, K. E.; Lin, W. *J. Am. Chem. Soc.* **2011**, *133*, 2056. (j) Pachfule, P.; Panda, M. K.; Kandambeth, S.; Shivaprasad, S. M.; Díaz, D. D.; Banerjee, R. *J. Mater. Chem. A* **2014**, *2*, 7944. (k) Pachfule, P.; Kandambeth, S.; Díaz, D. D.; Banerjee, R. *Chem. Commun.* **2014**, *50*, 3169.
- (15) Cooper et al. synthesized isomeric cage compound from (*R,R*)-1,2-diaminocyclohexane and tris(4-formylphenyl)amine in dichloromethane. Jelfs, K. E.; Wu, X.; Schmidtmann, M.; Jones, J. T. A.; Warren, J. E.; Adams, D. J.; Cooper, A. I. *Angew. Chem., Int. Ed.* **2011**, *50*, 10653.
- (16) (a) Grundmann, C. *Houben-Weyl: Methoden der Organischen Chemie*, 4th ed.; Thieme: Stuttgart, Germany, 1985; Vol. E5. (b) Kleemann, A.; Engel, J.; Kutscher, B.; Reichert, D. *Pharmaceutical Substances: Syntheses, Patents, Applications*, 5th ed.; Thieme: Stuttgart, Germany, 2009. (c) Sanderson, P. E. J.; Lyle, T. A.; Cutrona, K. J.; Dyer, D. L.; Dorsey, B. D.; McDonough, C. M.; Naylor-Olsen, A. M.; Chen, I. W.; Chen, Z.; Cook, J. J.; Cooper, C. M.; Gardell, S. J.; Hare, T. R.; Krueger, J. A.; Lewis, S. D.; Lin, B.; Lucas, J.; Lyle, E. A.; Lynch, J. J.; Stranieri, M. T.; Vastag, K.; Yan, Y.; Shafer, J. A.; Vacca, J. P. *J. Med. Chem.* **1998**, *41*, 4466.
- (17) (a) Sandmeyer, T. *Ber. Dtsch. Chem. Ges.* **1884**, *17*, 1633. (b) Hodgson, H. H. *Chem. Rev.* **1947**, *40*, 251. (c) Galli, C. *Chem. Rev.* **1988**, *88*, 765. (d) Mowry, D. T. *Chem. Rev.* **1948**, *42*, 189.
- (18) (a) Anbarasan, P.; Schareina, T.; Beller, M. *Chem. Soc. Rev.* **2011**, *40*, 5049. (b) Schareina, T.; Zapf, A.; Beller, M. *Chem. Commun.* **2004**, 1388. (c) Sundermeier, M.; Zapf, A.; Beller, M. *Eur. J. Inorg. Chem.* **2003**, *2003*, 3513. (d) Zanon, J.; Klapars, A.; Buchwald, S. L. *J. Am. Chem. Soc.* **2003**, *125*, 2890. (e) Weissman, S. A.; Zewge, D.; Chen, C. *J. Org. Chem.* **2005**, *70*, 1508. (f) Ushkov, A. V.; Grushin, V. V. *J. Am. Chem. Soc.* **2011**, *133*, 10999. (g) Arvela, R. K.; Leadbeater, N. E. *J. Org. Chem.* **2003**, *68*, 9122. (h) Cristau, H. J.; Ouali, A.; Spindler, J. F.; Taillefer, M. *Chem. - Eur. J.* **2005**, *11*, 2483. (i) Schareina, T.; Zapf, A.; Magerlein, W.; Müller, N.; Beller, M. *Chem. - Eur. J.* **2007**, *13*, 6249. (j) Ren, Y.; Wang, W.; Zhao, S.; Tian, X.; Wang, J.; Yin, W.; Cheng, L. *Tetrahedron Lett.* **2009**, *50*, 4595. (k) Senecal, T. D.; Shu, W.; Buchwald, S. L. *Angew. Chem., Int. Ed.* **2013**, *52*, 10035. (l) Yang, C.; Williams, J. M. *Org. Lett.* **2004**, *6*, 2837. (m) Zhang, J.; Chen, X.; Hu, T.; Zhang, Y.; Xu, K.; Yu, Y.; Huang, J. *Catal. Lett.* **2010**, *139*, 56. (n) Yeung, P. Y.; So, C. M.; Lau, C. P.; Kwong, F. Y. *Angew. Chem., Int. Ed.* **2010**, *49*, 8918. (o) Yeung, P. Y.; So, C. M.; Lau, C. P.; Kwong, F. Y. *Org. Lett.* **2011**, *13*, 648. (p) Yeung, P. Y.; So, C. M.; Lau, C. P.; Kwong, F. Y. *Tetrahedron Lett.* **2011**, *52*, 7038.
- (19) Frisch, M. J.; Trucks, G. W.; Schlegel, H. B.; Scuseria, G. E.; Robb, M. A.; Cheeseman, J. R.; Scalmani, G.; Barone, V.; Mennucci, B.; Petersson, G. A.; Nakatsuji, H.; Caricato, M.; Li, X.; Hratchian, H. P.; Izmaylov, A. F.; Bloino, J.; Zheng, G.; Sonnenberg, J. L.; Hada, M.; Ehara, M.; Toyota, K.; Fukuda, R.; Hasegawa, J.; Ishida, M.; Nakajima, T.; Honda, Y.; Kitao, O.; Nakai, H.; Vreven, T.; Montgomery, J. A., Jr.; Peralta, J. E.; Ogliaro, F.; Bearpark, M.; Heyd, J. J.; Brothers, E.; Kudin, K. N.; Staroverov, V. N.; Kobayashi, R.; Normand, J.; Raghavachari, K.; Rendell, A.; Burant, J. C.; Iyengar, S. S.; Tomasi, J.; Cossi, M.; Rega, N.; Millam, J. M.; Klene, M.; Knox, J. E.; Cross, J. B.; Bakken, V.; Adamo, C.; Jaramillo, J.; Gomperts, R.; Stratmann, R. E.; Yazyev, O.; Austin, A. J.; Cammi, R.; Pomelli, C.; Ochterski, J. W.; Martin, R. L.; Morokuma, K.; Zakrzewski, V. G.; Voth, G. A.; Salvador, P.; Dannenberg, J. J.; Dapprich, S.; Daniels, A. D.; Farkas, O.; Foresman, J. B.; Ortiz, J. V.; Cioslowski, J.; Fox, D. J. *Gaussian 09*, Revision A.02; Gaussian, Inc.: Wallingford, CT, 2009.
- (20) Becke, A. D. *Phys. Rev. A: At., Mol., Opt. Phys.* **1988**, *38*, 3098.
- (21) Lee, C.; Yang, W.; Parr, R. G. *Phys. Rev. B: Condens. Matter Mater. Phys.* **1988**, *37*, 785.
- (22) SMART/SAINT; Bruker AXS, Inc.: Madison, WI, 2004.
- (23) Sheldrick, G. M. *SHELX-97*; University of Göttingen: Göttingen, Germany, 1998.
- (24) Farrugia, L. J. *J. Appl. Crystallogr.* **1999**, *32*, 837. Farrugia, L. J. *WinGX*, version 1.65.04; Department of Chemistry, University of Glasgow: Glasgow, Scotland, 2003.
- (25) Sheldrick, G. M. *SADABS*; University of Göttingen: Göttingen, Germany, 1999.